



GEORGIA INSTITUTE OF TECHNOLOGY

AE 4699

UNDERGRADUATE RESEARCH

NACA 23012 Fluent Analysis

Author:

Max Geissbuhler

Student Number:

*****647

February 17, 2019

Contents

1	Fluent Setup	2
1.1	Geometry	2
1.2	Meshing	3
1.3	Fluent	5
2	Fluent Results	6
2.1	0° Angle of Attack	6
2.2	2° Angle of Attack	8
2.3	4° Angle of Attack	10
2.4	6° Angle of Attack	12
2.5	8° Angle of Attack	14
3	Abbot and Doenhoff Results [1]	16
4	Comparison of Results	17

1 Fluent Setup

1.1 Geometry

The first step in running the analysis on the NACA 23012 wing was to input the geometry of the wing into the DesignModeler application within ANSYS Workbench. The geometry of the wing was taken from a 3D model, which was converted from a .STL file to a .STEP file in SolidWorks. Once the geometry was input into DesignModeler, a coordinate system was created, with the origin placed at the trailing edge of the airfoil (this would make meshing take less time). Then, a 180° arc with a radius of 12.5 meters was placed with its focus at the origin. After the arc was created, a rectangle was placed with a width of 12 meters, connected to the endpoints of the arc. The arc and the rectangle would serve as the inlet and outlet of the system and would allow for the mesh to be created in such a way that the most detailed portion would be at the origin, where the airfoil is located. Figure 1 shows the geometry model within DesignModeler.

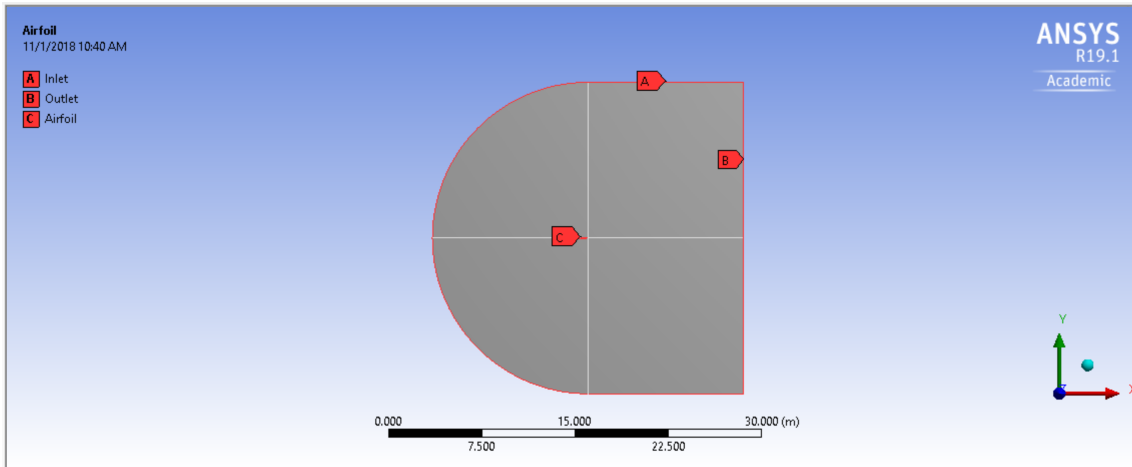


Figure 1: Geometry Used in Analysis

1.2 Meshing

Following this step, the geometry file was imported into the Mesh Editor in Workbench. While pursuing the most accurate data, two meshing methods were pursued, and the method with the most accurate data was ultimately selected to report the data in this report. In the first method, face mapping and edge sizing were selected within the mesh editor. For the edge sizing, an edge bias was selected so that the most detail in the mesh would be located in the center of the mesh, where the airfoil is. Originally, the number of divisions for each edge sizing was selected to be 100, but this number was later increased to 200 divisions to increase the quality of the mesh. After running this mesh in Fluent, it became evident that the mesh was less accurate than the mesh created using the second method, so the 2nd method mesh was ultimately used to collect the data in this report. The second meshing method used a body sizing with a sphere of influence originating at the leading edge of the airfoil and with a radius of 1.3 meters, and an element size of 0.025 meters. An edge sizing was also selected on the airfoil, with 1000 divisions selected. Finally, an inflation was placed on the airfoil, with 20 divisions and a maximum thickness of 0.01 meters. Figures 3 and 2 show the mesh within the Mesh Editor.

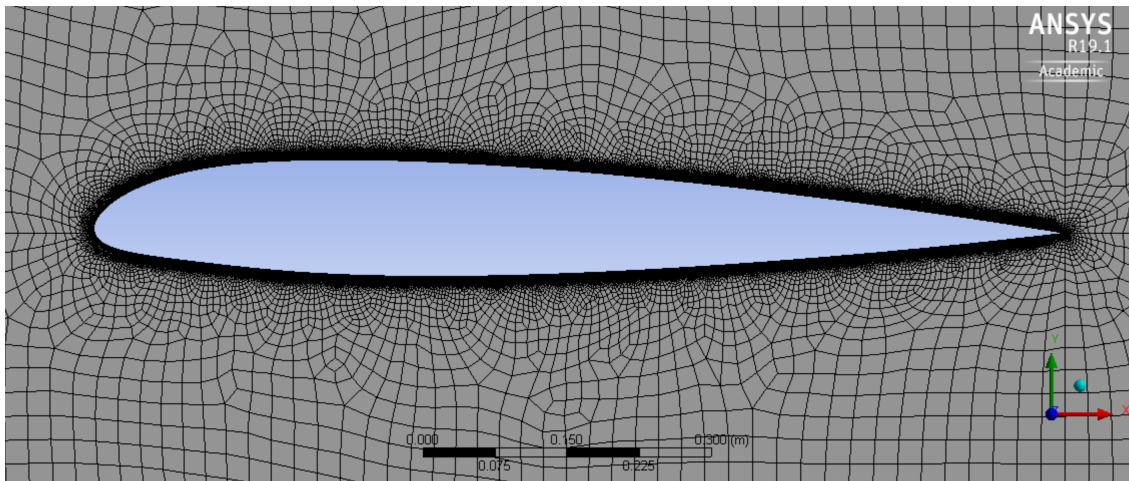


Figure 2: Airfoil Within Mesh

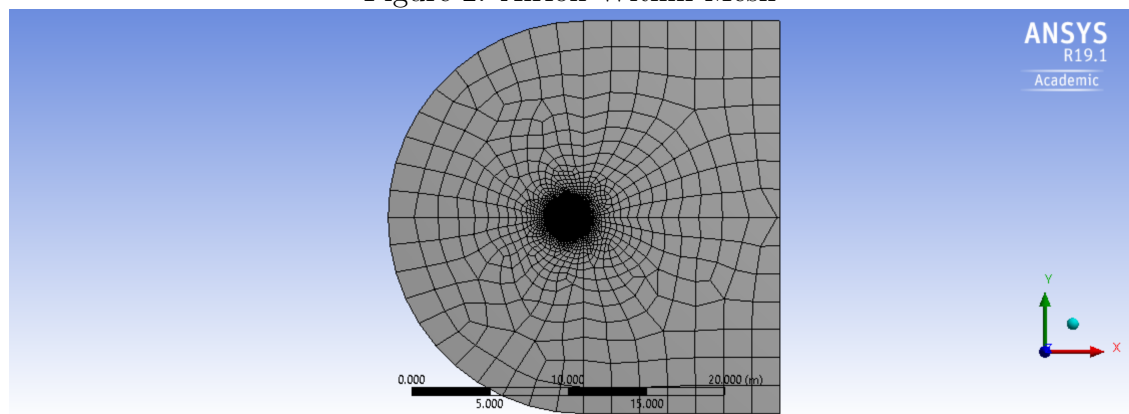


Figure 3: Complete View of C Mesh

1.3 Fluent

The next phase of the modelling was the Fluent phase. After importing the mesh into Fluent, the models were selected. For the calculations shown in this report, a density-based design was used with energy activated and an SST k-omega viscous model. Using the ideal gas law, the density of air was selected to be $1.246697 \frac{kg}{m^3}$. C_p was selected to be $1006.43 \frac{j}{kg*k}$ and thermal conductivity was selected to be $0.0242 \frac{W}{m*k}$. Using the definition of the Reynold's Number, $Re = \frac{\rho_\infty v_\infty c}{\mu_\infty}$, and the knowledge that a Reynold's Number of 3,000,000 was required for our simulation, viscosity was calculated to be $1.419233 * 10^{-7} \frac{kg}{m*sec}$. The operating conditions were selected to be 101.325 kPa and 283.15 K. The boundary conditions were reset for each trial, as the inlet velocity and its components determine the effective angle of attack of the airfoil. The components of the velocity were calculated by using $\cos(\alpha)$ for the x-component, and $\sin(\alpha)$ for the y- component. A velocity value of $34 \frac{m}{sec}$ was used for the inlet. This value was calculated by finding the speed of sound using $a = \sqrt{\gamma RT}$, and then multiplying by 0.1 (the selected Mach number for this analysis). The turbulence was set to 1 % and the turbulent viscosity ratio set to 1 in order to model the mostly laminar flow present in the controlled conditions of a wind tunnel. The reference values were calculated from the inlet, and the reference area was set to $1 m^2$ and the reference length and width set to 1 m. The solution method for this analysis was chosen to be an Implicit Roe FDS Green-Gauss Node Based model. The flow, turbulent kinetic energy, and specific dissipation rate were simulated as 2nd order upstream systems. A standard initialization was calculated from the inlet prior to solving. Finally, 1000 iterations were selected with subsonic solution steering activated.

Air Parameter	Value	Operating Condition	Value
Density	$1.246697 \frac{kg}{m^3}$	Temperature	283.15 k
C_p	$1006.43 \frac{j}{kg*k}$	Pressure	101.325 kPa
Thermal Conductivity	545	Reynold's Number	3 E6
μ_∞	545		

Velocity Param.	Value	Solution Param.	Value
Magnitude	$34 \frac{m}{sec}$	Formulation	Implicit
X-Component	$1006.43 \frac{j}{kg*k}$	Flux Type	Roe-FDS
Y-Component	545	Gradient	Green-Gauss Node Based
		Flow	2 nd Order Upwind
		Turbulent K.E.	2 nd Order Upwind
		Spec. Diss. Rate	2 nd Order Upwind

2 Fluent Results

α	C_L	C_D	C_M
0°	0.13256	0.00549	-0.00876
2°	0.35836	0.00603	-0.00992
4°	0.58356	0.00712	-0.01101
6°	0.80434	0.00902	-0.01192
8°	1.02279	0.01149	-0.01266

2.1 0° Angle of Attack

At an α of 0°, Fluent yielded a C_L value of 0.13256, a C_D of 0.00549, and a C_M of -0.00876. The non-zero value of C_L is sensible given that the NACA 23012 wing is asymmetric. Additionally, by using the extension of the Kutta-Jukowski Theorem $C_L \approx 2\pi(\alpha - \alpha_0)$ [2] and that $\alpha_0 = -1.80^\circ$ [1], an approximation of the expected coefficient of lift is 0.1974. Thus, Fluent generated a reasonable coefficient of lift. As the airfoil was simulated with minimal turbulence, an approximation of the skin friction drag in laminar flow can be given as $C_f = 2^{\frac{1.328}{\sqrt{Re}}}$, which yields a net value of 0.00153, while an approximation of skin friction drag in turbulent flow can be given as $C_f = 2^{\frac{0.074}{Re^{1/5}}} = 0.00750$ [2]. Comparing the Fluent generated drag coefficient to these approximations, it falls in between both approximations as would be expected. From Figure 4, it is evident that the stagnation point on the wing is on the leading edge of the airfoil, which is sensible given that the wing is at an angle of attack of 0°. Additionally, the flow along the upper surface of the wing is moving more quickly than the flow along the lower surface, as is expected. Finally, from Figures 5 and 6, it is apparent that the magnitude of pressure on the lower surface is greater than it is on the upper surface. In conclusion, Figures 4, 5, and 6 demonstrate that the airfoil satisfies Bernoulli's Principle and that our solution at this angle of attack is valid.

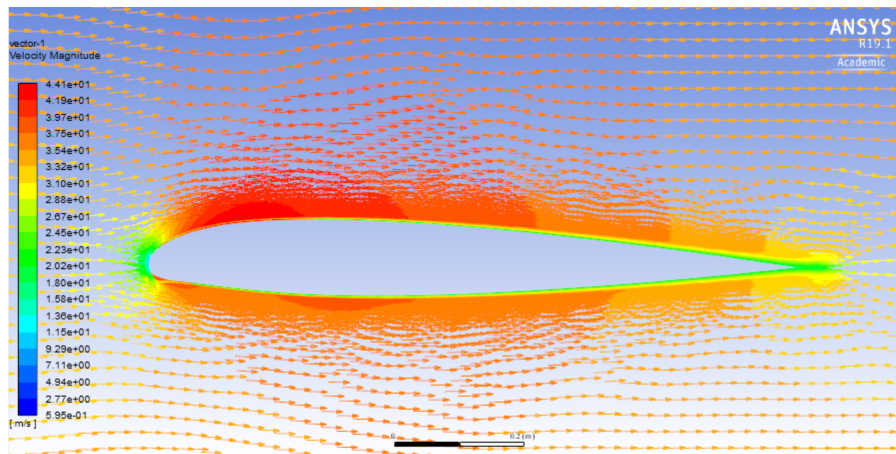


Figure 4: Velocity Magnitude Vector Plot

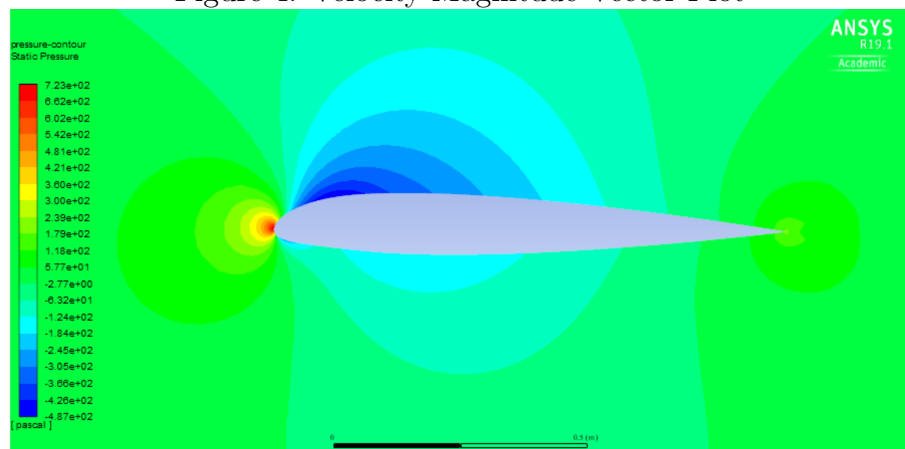


Figure 5: Pressure Magnitude Contour Plot

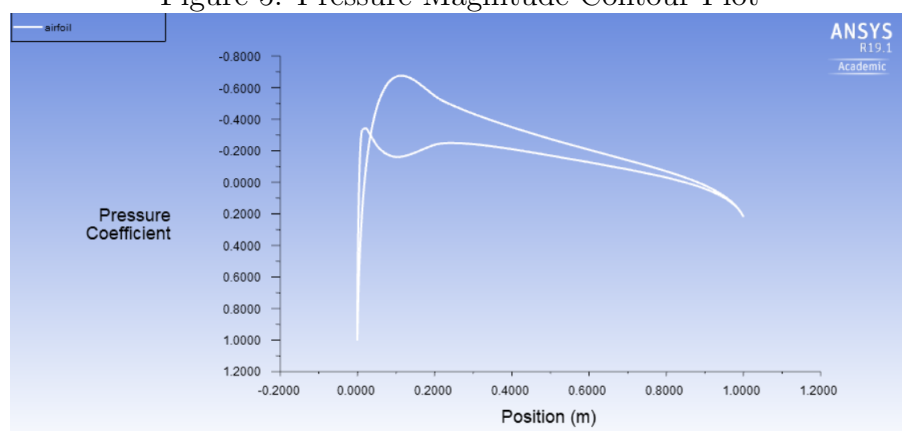


Figure 6: Coefficient of Pressure Over the Airfoil

2.2 2° Angle of Attack

At an α of 2°, Fluent yielded a C_L of 0.35836, a C_D of 0.00603, and a C_M of -0.00992. Using the extension of the Kutta-Jukowski Theorem, an estimate for the expected value of the coefficient of lift is 0.41672, which is within 16 % of the Fluent value. Referring to the flat plate skin friction estimations from section 2.1, the Fluent coefficient of drag value is in between the estimations. In Figure 7, it is evident that the airflow over the top of the wing is moving faster than the air below the wing, as was predicted. From Figure 8 the point at which the air impacts the wing can be seen slightly below the mean chord line of the wing, which makes sense given that the wing is at a slight angle of attack. Finally, Figure 9 shows the distribution of the coefficient of pressure along the wing, showing a higher value of c_p for the bottom side of the wing and a lower value of c_p for the top of the wing.

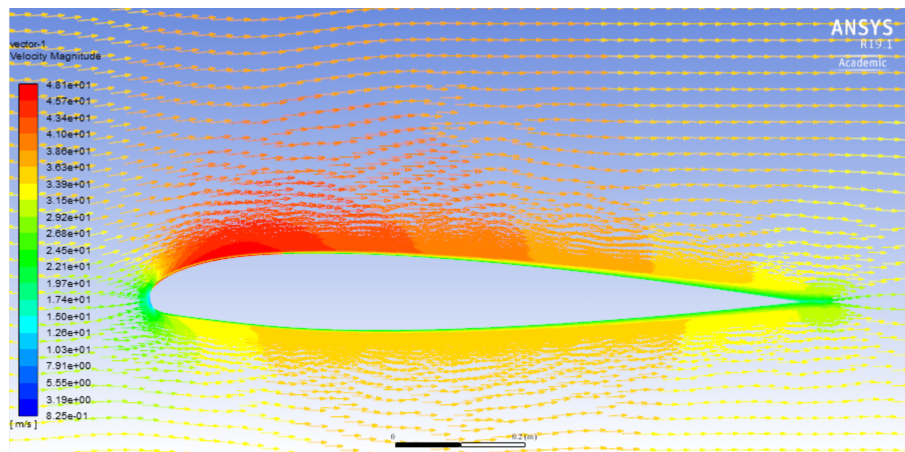


Figure 7: Velocity Magnitude Vector Plot

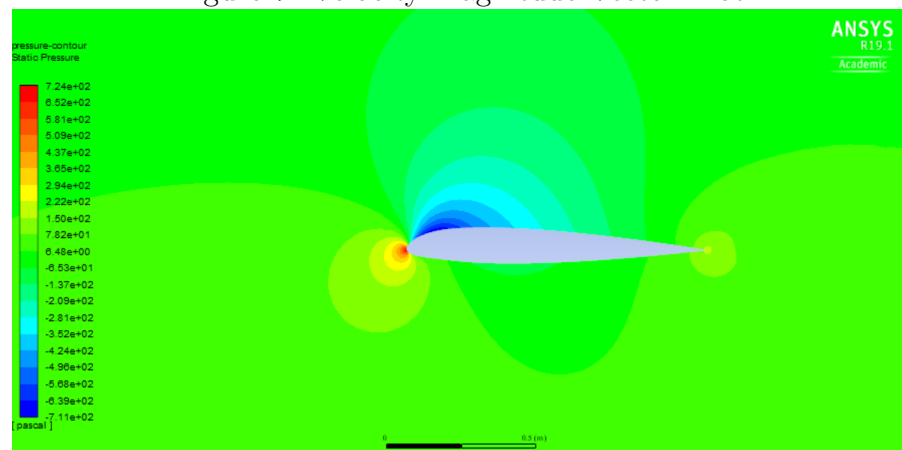


Figure 8: Pressure Magnitude Contour Plot

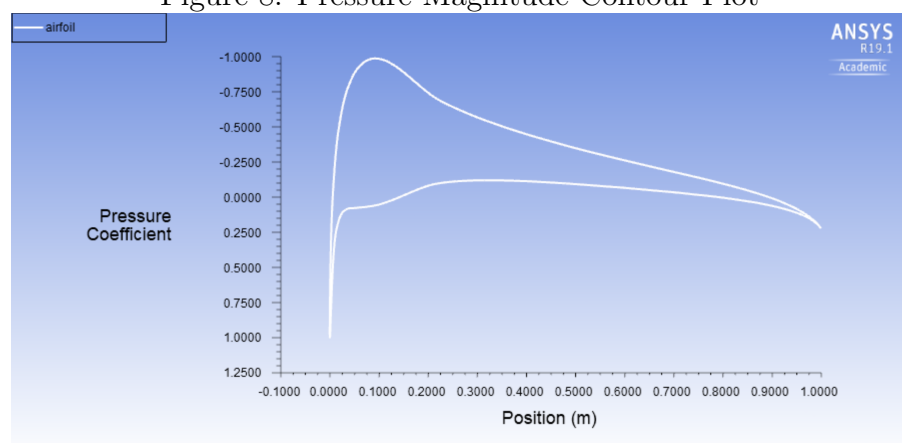


Figure 9: Coefficient of Pressure Over the Airfoil

2.3 4° Angle of Attack

At an α of 4° Fluent calculated a C_L of 0.58356, a C_D of 0.00712, and a C_M of -0.01101. Using the same approach as the previous sections, an ideal C_L value is 0.6360, a value that is within 8.99 % of the Fluent-generated value. Upon inspection of the estimates for skin friction drag (0.00153 for laminar flow and 0.00750 for turbulent flow), it is evident that the Fluent-generated C_D is within both estimates, while simultaneously closer to the turbulent flow estimate than the previous two drag values. This makes sense because drag is composed of skin friction drag, induced drag, and wave drag (which can be ignored since analysis is being performed at Mach 0.1). Induced drag increases as lift increases, so drag should increase as lift increases. In other words, the Fluent estimation of drag should approach and exceed the prediction of flat plate drag in laminar flow as the angle of attack (and thus lift) increase. Inspection of Figure 10 shows that the air is moving much more quickly over the upper surface of the wing than the bottom surface. Additionally, the stagnation point can be seen in dark blue slightly below the mean chord line on the leading edge of the wing. In Figure 11, the stagnation point stands out as the point about which the magnitude of pressure is highest. In Figure 12, the distance between the plots of C_P is greater than in Figures 6 and 8. This is to be expected, as this distance represents the C_L along the wing, and the wing is expected to generate more lift at 4° than at 0° or 2° .

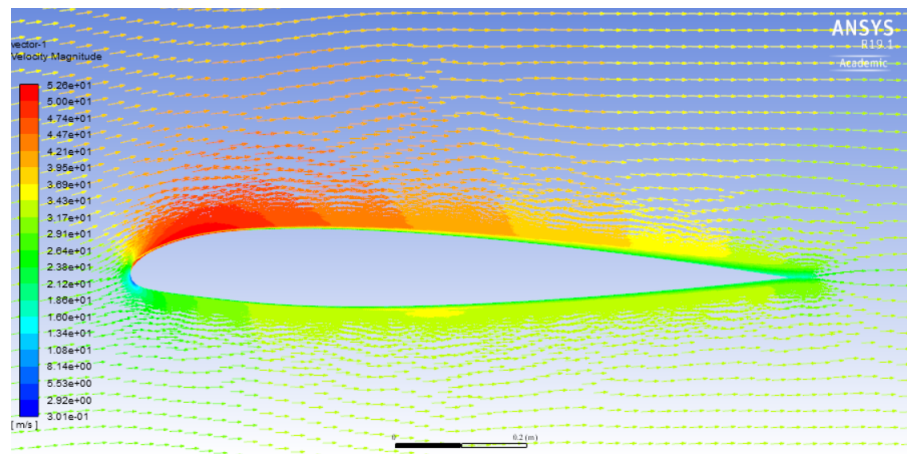


Figure 10: Velocity Magnitude Vector Plot

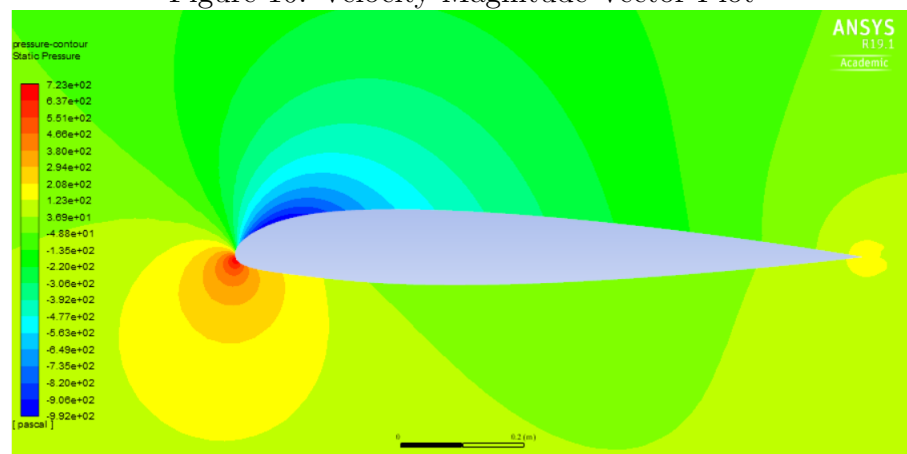


Figure 11: Pressure Magnitude Contour Plot

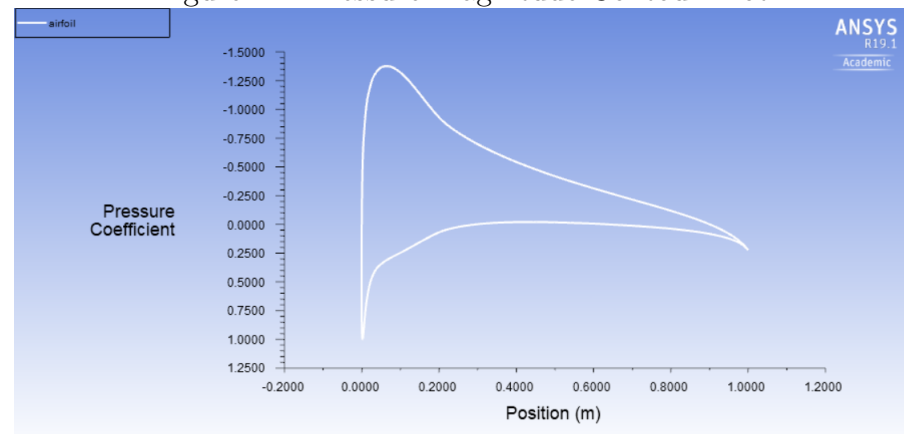


Figure 12: Coefficient of Pressure Over the Airfoil

2.4 6° Angle of Attack

At an α of 6° Fluent calculated a C_L of 0.80434, a C_D of 0.00902, and a C_M of -0.01192. The Kutta-Jukowski Extension yields a theoretical lift coefficient of 0.8554, a value that is within 6.34 % of the Fluent generated C_L . The drag coefficient at this angle of attack is larger than the flat plate estimate, as a result of lift induced drag and skin friction drag. Figure 13 shows that the air velocity along the bottom surface of the wing is nearly constant, while on the upper surface the air velocity is much greater at the leading edge and decreases along the wing. Figure 14 shows that the pressure along the upper surface is lower than the bottom of the wing. In particular, it shows a region roughly 0.125 m long along the upper surface of the wing near the leading edge where the magnitude of pressure is significantly lower than the pressure elsewhere along the wing. This is the result of the angle of attack, and after a certain angle, this region will grow large enough to allow for flow separation and stall to occur. Figure 15 confirms the numerical lift coefficient result, with a larger C_P separation between the upper and lower surfaces than at lower angles of attack.

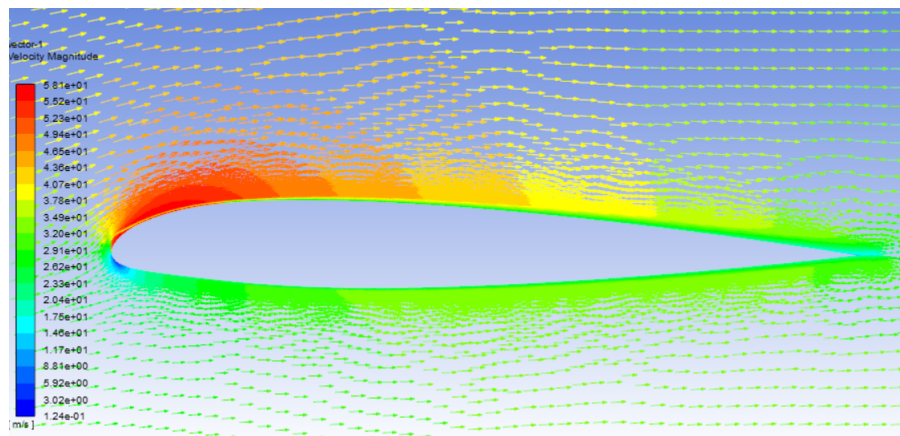


Figure 13: Velocity Magnitude Vector Plot

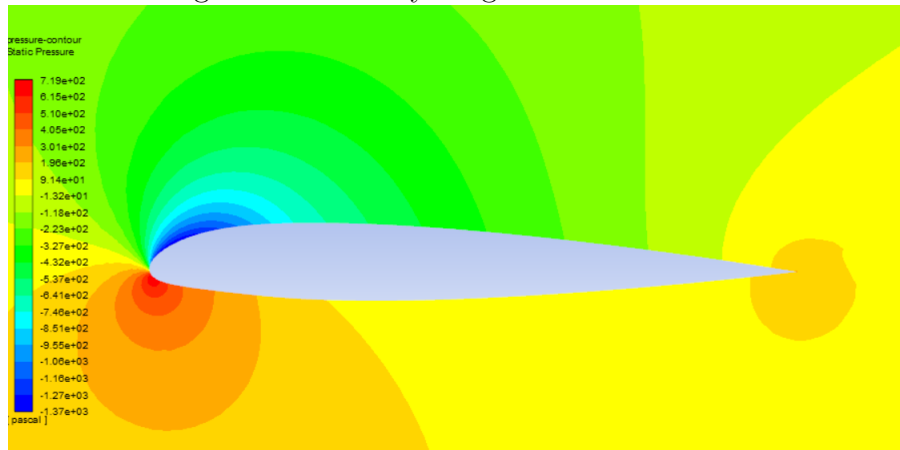


Figure 14: Pressure Magnitude Contour Plot

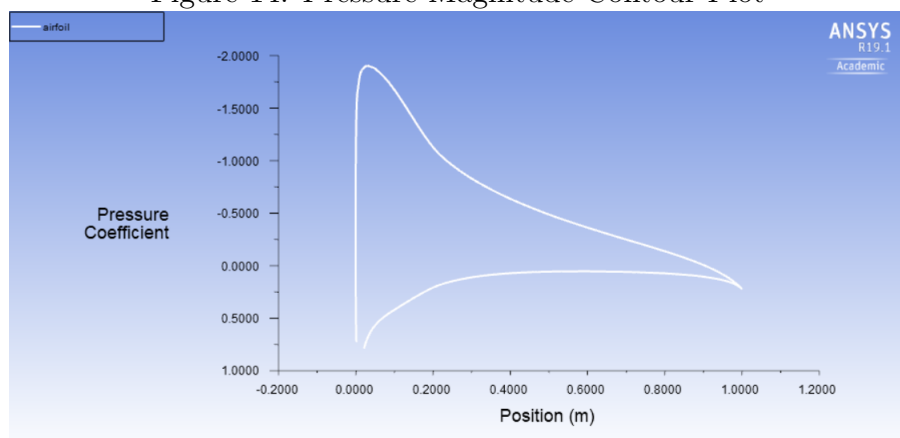


Figure 15: Coefficient of Pressure Over the Airfoil

2.5 8° Angle of Attack

At the final angle of attack of 8° Fluent computed a C_L of 1.02279, a C_D of 0.01149 and a C_M of -0.01266. Using the method outlined in Section 2.1, the theoretical C_L at this angle of attack is 1.0747, meaning that the Fluent generated value is within 5.07% of the theoretical value. The coefficient of drag is larger than the coefficient of drag at $\alpha = 6^\circ$ as is expected. Comparing the moment coefficient about $\frac{1}{4}$ chord across the range of α 's used in Fluent, it is evident that the value is nearly constant, as it is expected to be. Figure 16 shows that the magnitude of the air velocity is much higher along the upper surface of the wing, as it was for the other values of α . Figure 17 is similar to Figure 14 except that the disturbance created by the airfoil is larger at an 8° angle of attack, as the large yellow bubble above the upper surface shows. Finally, the graph of C_P along the wing in Figure 18 is of the expected shape and has the largest spread across the range of α 's between the upper and lower surface plots.

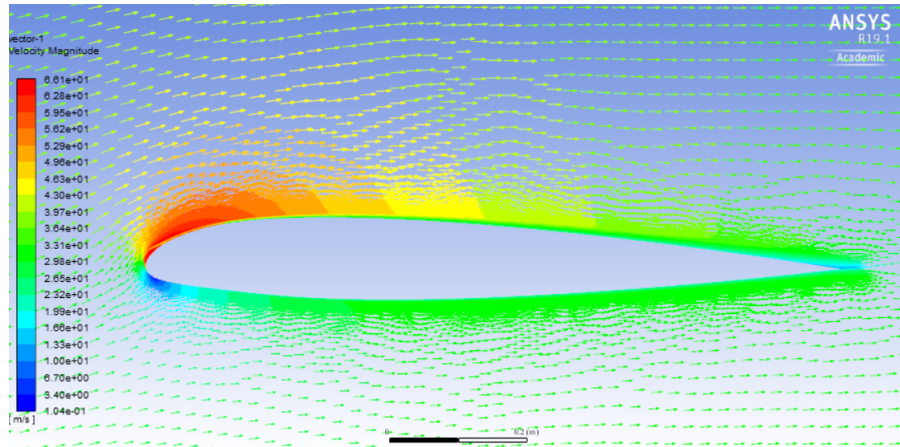


Figure 16: Velocity Magnitude Vector Plot

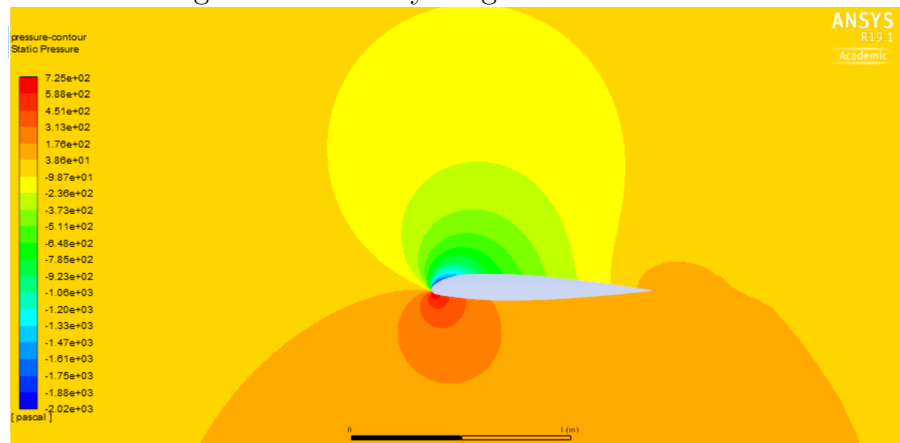


Figure 17: Pressure Magnitude Contour Plot

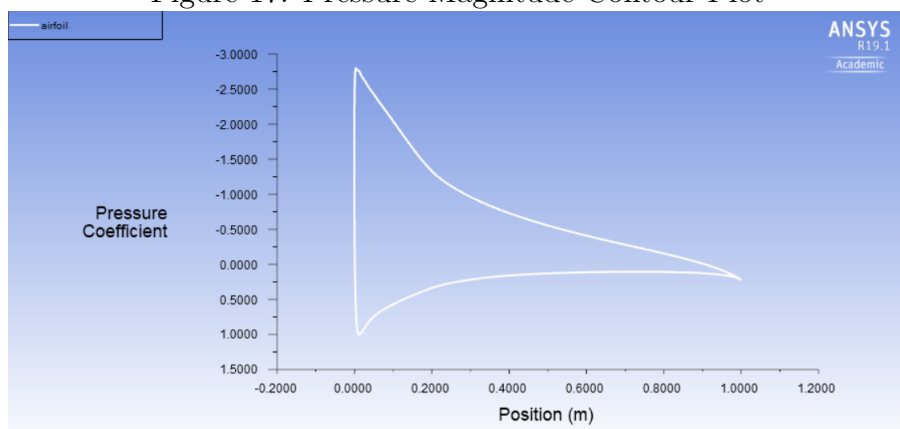


Figure 18: Pressure Magnitude Contour Plot

3 Abbot and Doenhoff Results [1]

α	C_L	C_D	C_M
0°	0.120	0.0069	-0.010
2°	0.320	0.0068	-0.010
4°	0.520	0.0070	-0.010
6°	0.750	0.0078	-0.010
8°	0.970	0.0089	-0.010

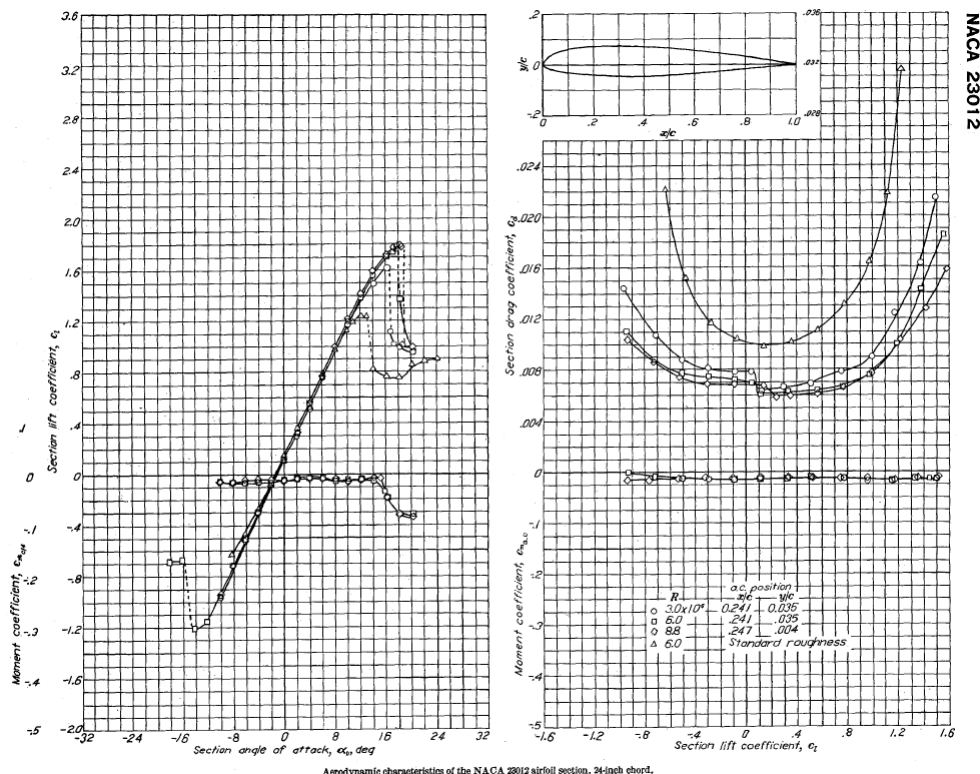


Figure 19: Abbot and Doenhoff Plots of C_L vs. α and Drag Polar for NACA 23012 Airfoil

4 Comparison of Results

Overall, Fluent was accurate in its estimations of the lift, drag, and moment across the range of angles of attack from 0° to 8° . The table below shows the error between the Fluent data and the published NACA data. From the table, it is evident that the average error across all three parameters is less than 16%. The error in the calculated coefficient of lift is lower than the error in the calculated drag and moment. The error in C_D is the largest as it would be expected. It is expected to be larger because calculating skin friction drag is a complicated process, and the airfoil is simplified in the meshing process, reducing the accuracy of the calculated value. The error in the calculated value of the pitching moment about $\frac{1}{4}$ chord decreases as the other values become more accurate, and increases as the other values become less accurate. This also makes sense, as the pitching moment is the result of aerodynamic forces acting on the airfoil, and a less accurate estimation of C_D should make a calculation of aerodynamic forces less accurate.

In conclusion, the data produced by Fluent closely resembles the data published in the Summary of Airfoil Data report. The Fluent data is not a perfect match of the published data, but it is (on average) within 16% of the published data.

α	C_L Error	C_D Error	C_M Error
0°	10.470%	20.390%	12.379%
2°	11.988%	11.289%	0.830%
4°	12.224%	1.778%	10.113%
6°	7.245%	15.669%	19.172%
8°	5.442%	29.124%	26.650%
AVG.	9.474%	15.650%	13.829%

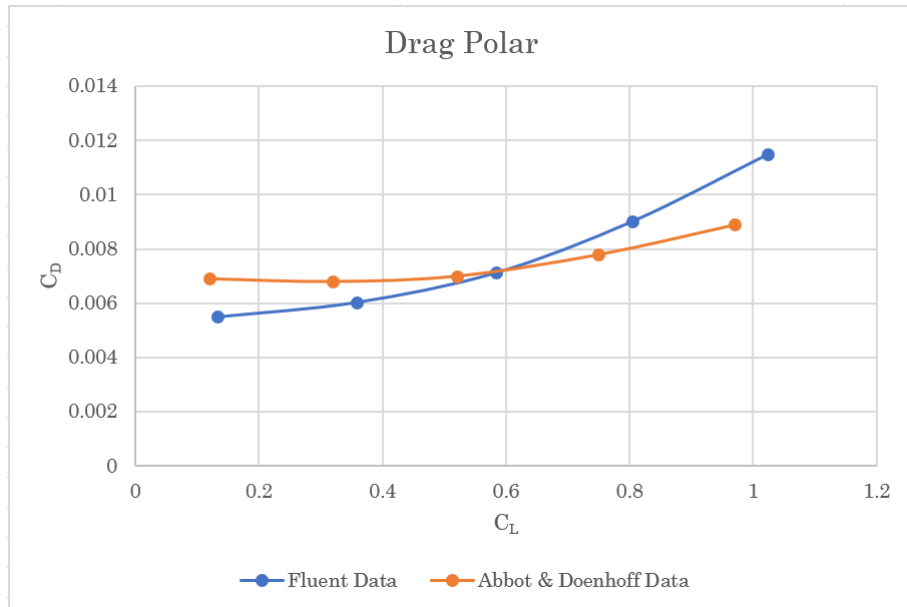
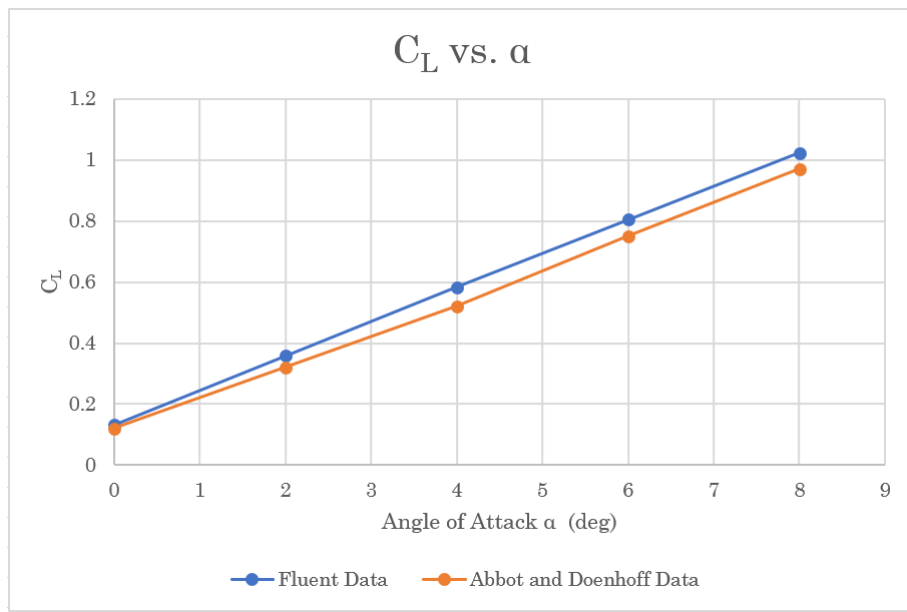


Figure 20: Drag Polar Comparison

Figure 21: C_L Comparison

References

- [1] Ira H. Abbott, Albert E. von Doenhoff, and Louis S. Stivers Jr. Summary of airfoil data. Technical report, National Advisory Committee for Aeronautics, 1945.
- [2] John D. Anderson Jr. *Fundamentals of Aerodynamics, 5th Edition*. McGraw-Hill, 2011.